Aligned Carbon Nanotube Film Enables Thermally Induced State Transformations in Layered Polymeric Materials

Citation: Lee, Jeonyoon et al. "Aligned Carbon Nanotube Film Enables Thermally Induced State Transformations in Layered Polymeric Materials." ACS Applied Materials & Interfaces 7, 16 (April 2015): 8900–8905 © 2015 American Chemical Society

As Published: http://dx.doi.org/10.1021/acsami.5b01544

Publisher: American Chemical Society (ACS)

Persistent URL: http://hdl.handle.net/1721.1/112326

Version: Author's final manuscript: final author's manuscript post peer review, without publisher's formatting or copy editing

Aligned Carbon Nanotube Film Enables Thermally Induced State Transformations in Layered Polymeric Materials

Jeonyoon Lee,[†,‡] Itai Y. Stein,[†,‡] Seth S. Kessler,[¶] and Brian L. Wardle[*,§]

E-mail: wardle@mit.edu

[*]To whom correspondence should be addressed

[†]Department of Mechanical Engineering, Massachusetts Institute of Technology, 77 Massachusetts Ave, Cambridge, Massachusetts 02139, USA.

[‡]These authors have contributed equally to this work

[¶]Metis Design Corporation, 205 Portland St, Boston, Massachusetts 02114, USA.

[§]Department of Aeronautics and Astronautics, Massachusetts Institute of Technology, 77 Massachusetts Ave, Cambridge, MA 02139, USA

Abstract

The energy losses and geometric constraints associated with conventional curing techniques of polymeric systems motivate the study of a highly scalable out-of-oven curing method using a nanostructured resistive heater comprised of aligned carbon nanotubes (A-CNT). The experimental results indicate that, when compared to conventional oven-based techniques, the use of an "out-of-oven" A-CNT integrated heater leads to orders of magnitude reductions in the energy required to process polymeric layered structures such as composites. Integration of this technology into structural systems enables the *in situ* curing of large-scale polymeric systems at high efficiencies, while adding sensing and control capabilities.

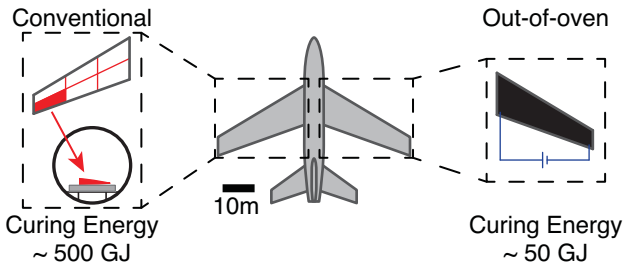

Keywords: Carbon nanotubes, Resistive heating, Hybrid materials, Polymer composites, Manufacturing

1 Introduction

Polymeric materials whose structure and properties can be precisely and reversibly engineered using external stimuli, such as heat,[1–5] light,[2–4] etc., are prime candidates for use in many high value applications including self-healing/re-healing materials,[1–6] sensors and actuators,[1,4] electronic skin,[4] and structural components.[1–3] While heat is one of the most accessible and widely used type of stimuli,[1,3,4] the introduction of heat into a complex polymeric structure or device in an efficient and direct manner is difficult, and requires the effective integration of small form-factor heaters into the polymeric architectures.[4] This can be achieved using microheater films. Using nanoscale elements, such as carbon nanotubes (CNTs),[7–22] graphene,[10,20–23] metal nanowires (NWs),[19,24–31] or hybrids of thereof,[24,32] recent work has shown that microheater films with high operating temperatures and fast thermal ramp rates can be made. However, the lack of CNT/graphene/NW alignment in these microheater films compromises their mechanical properties and electrical stability,[32] making them less suitable for application in structures that may be exposed to stress, such as airplane wings.

Recent work on A-CNT networks showed that microheaters made *via* roller densification of A-CNT arrays are highly scalable,[33–36] and have tunable electron transport properties.[34–37] Additionally, the low density of these films,[34] which originates from the CNT intrinsic density and volume fraction,[38] makes them ideal for applications requiring a lightweight integrated microheater film, such as *in situ* deicing and heat treatment of airplane wings.[39] However, while these previous studies explored the physics underlying electron transport in the A-CNT networks, they did not explore the performance of these films as microheaters in realistic operating conditions. Here we study the performance of A-CNT networks as microheaters, and show that these films can enable highly efficient manufacturing of effective structural elements for next-generation material architectures.

To evaluate the use of A-CNT networks as integrated heating elements for large structures, A-CNT networks were used to heat treat a polymer matrix composite (PMC) com-

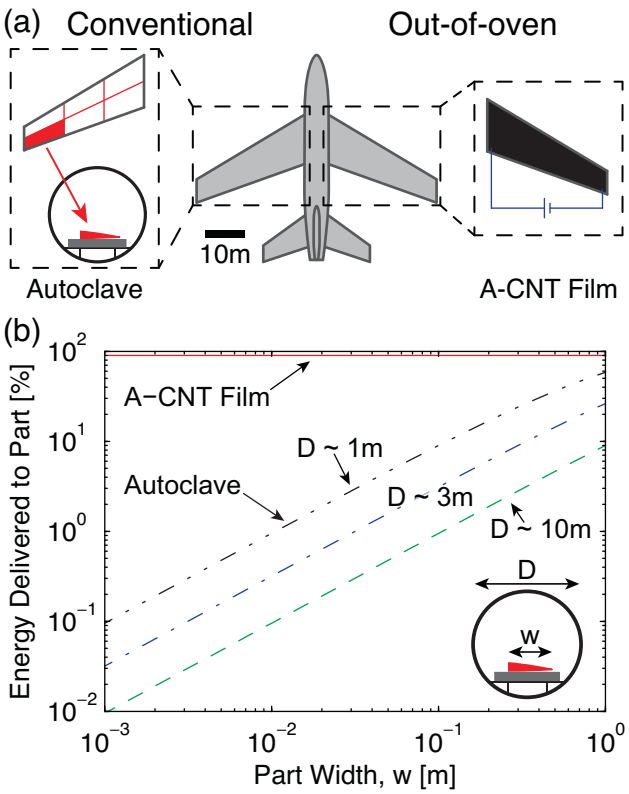

Figure 1: Comparison of conventional and out-of-oven manufacturing techniques. (a) Illustration of the key differences between conventional (autoclave) and aligned carbon nanotube (A-CNT) film out-of-oven curing techniques. (b) Comparison of the amount of energy delivered to the composite structure as a function of the amount of energy in showing orders of magnitude reductions in energy required for manufacturing.

monly used in aerospace architectures. While such materials are normally processed using a geometrically constrained autoclave or similar oven based technique, here we show that an integrated microheater film can be used to heat treat the PMCs *in situ* regardless of the part size and shape (see Figure 1a for an illustration of the two manufacturing techniques, the latter termed "out-of-oven"). Since the integrated heating film directly and efficiently transfers heat *via* conduction, whereas conventional oven based manufacturing techniques indirectly and inefficiently transfer heat *via* convection through a gas medium, the integration of an A-CNT network based microheater can significantly reduce, by orders of magnitude, the energy consumed during manufacturing of PMCs. See Figure 1b for a plot illustrating the percentage of input heat energy that was transferred to the part being manufactured

for the conventional (oven-based), and A-CNT film based manufacturing techniques. This order of magnitude analysis consisted of a 2D Biot-like comparison of two convective thermal resistances assuming imperfect insulation: the ratio of the total thermal resistance from the wall to the part and the convective thermal resistance of the oven assuming that the ratio of the temperature differences between the wall and the part (ΔT_{wp}) and the wall and the gas (ΔT_{wg}) is constant ($\rightarrow \Delta T_{\mathrm{wp}}/\Delta T_{\mathrm{wg}} \sim 1.5$ for a wall temperature of ~ 500°C, gas temperature of ~ 300°C, and part temperature of ~ 200°C), and that one of the heater and oven dimensions is matched (a 3D $\rightarrow$ 2D simplification); the ratio of the conductive thermal resistance from the heater to the part in a one-sided curing setup (see Figure 2 for illustration) and the convective thermal resistance from the heater to the ambient gas. As Figure 1b shows, the A-CNT microheater based technique transfers $\sim 90\%$ of the input energy to the part regardless of the part width, whereas the fraction of energy transferred to the part in the oven based techniques depends on the part width and oven size (to first order) and peaks at $\sim 50\%$ when the part size is matched to the oven dimensions. Additional energy savings may be realized in the oven-based techniques by utilizing microwave heating,[40,41] which also achieves a more uniform thermal distribution inside of the part relative to oven or autoclave curing,[40–43] but is limited by the interaction of the part with microwave radiation and of course requires microwave generation and shielding.[40] Reductions in cure cycle duration could also be realized in the out-of-oven technique by utilizing the fast ramp rate of the A-CNT film heater, which can exceed 1°C/s,[21] in conjunction with their enhanced heat delivery mechanism. Through an analysis of the degree of cure of the PMC, we demonstrate that integrated A-CNT network based microheaters can be effectively and efficiently (as above) used for *in situ* heat treatment to manufacture (*i.e.* cure) structural components.

Since the sheet resistance of A-CNT networks synthesized *via* roller densification of A-CNT arrays is inversely proportional to the length of the enclosed CNTs,[37] and because a lower sheet resistance enables more electric energy to be dissipated as heat at a given operating voltage,[21] the A-CNT networks used here were comprised of long ($\gtrapprox 300$ μm) CNTs.

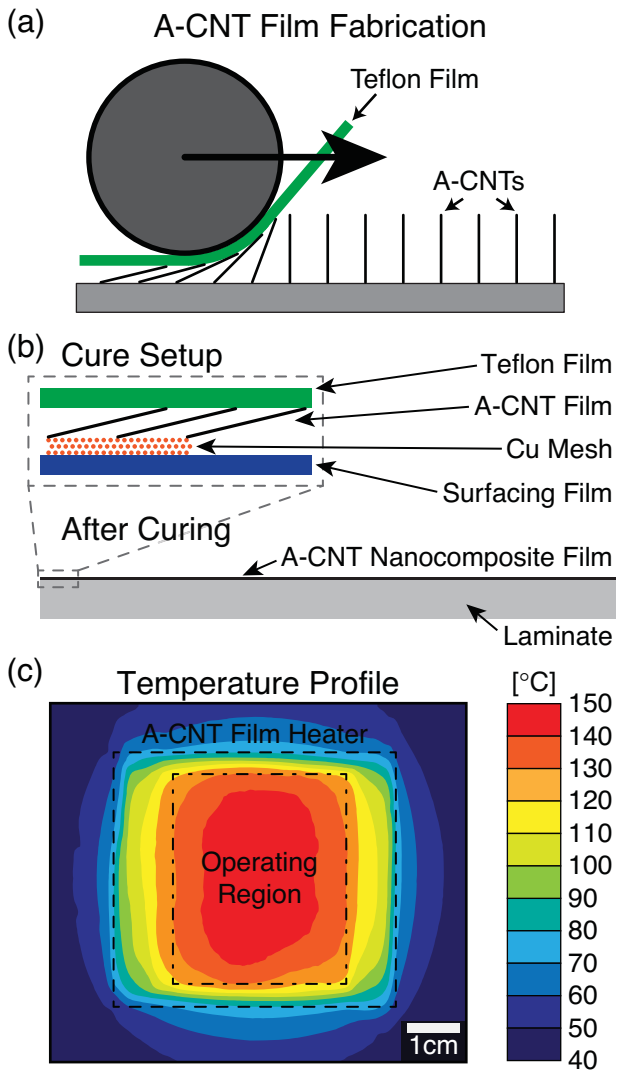

Figure 2: Synthesis and testing methods. (a) Illustration of the synthesis process of aligned carbon nanotube (A-CNT) films from A-CNT arrays *via* rolling densification. (b) Side view schematic of the A-CNT film heater, and the one-sided curing setup used in this study. (c) In-plane thermograph of the A-CNT film heater operating at ~ 150°C demonstrating spatial variation in temperature of $\lessapprox 15$°C in the operating region.

See Figure 2a for an illustration of the roller densification process. These A-CNT films were then joined with Cu mesh electrodes, for electrical contact, and a surfacing film, for electrical but not thermal insulation, forming a ~ 100 μm thick microheater film. See Figure 2b for an illustration of the microheater film, and the setup used to test the microheater performance *via* the heat treatment of a PMC. This manufacturing technique minimizes spatial inhomogeneities, and ensures that the resulting microheater film exhibits no hot spots and

has a precisely controllable operating temperature. See Figure 2c for a thermogram of the microheater film at a target temperature of 150°C with deviations of $\lessapprox$ 15°C. Using this microheater film, we show that a commercial laminated composite, Cycom 5320-1 unidirectional carbon fiber thermoset prepreg in a 0° layup with fibers aligned with the direction of current flow between electrodes (matching the alignment of the CNTs), used in aerospace structures can be effectively processed outside of an oven.

2 Materials and Methods

Composite Fabrication and Processing. A-CNT arrays were grown in a 44 mm internal diameter quartz tube furnace at atmospheric pressure *via* a thermal catalytic chemical vapor deposition process, very similar to a previously described process,[44–46] with ethylene as the carbon source and 600 ppm of water vapor added to the inert gas. The CNTs were grown on 40 mm × 50 mm Si substrates forming A-CNT arrays that are $\gtrapprox$ 300 μm tall, and are composed of multiwalled CNTs that have an average outer diameter of $\approx$ 7.8 nm ($3-7$ walls[47] with an average inner diameter of $\approx$ 5.1 nm),[37] evaluated intrinsic CNT density of $\approx$ 1.6 g/cm^3,[37,38] average inter-CNT spacing of $\approx$ 59 nm, and corresponding volume fraction of $\approx$ 1.6% CNTs.[37,46,48] The A-CNTs were re-oriented horizontally and densified using a 10 mm diameter rod and Guaranteed Nonporous Teflon (GNPT) film by rolling in the desired alignment directions (see Figure 2a for illustration). Since the post-growth H_2 anneal step weakens the attachment of the CNTs to the catalyst layer,[49] the A-CNT film adheres to the GNPT film and is cleanly removed from the Si substrate.

To assemble the A-CNT heater, two mesh electrodes made using Cu mesh (2CU4-100FA from Dexmet, Inc.) were first attached to a composite surfacing film (TC235-1SF from TenCate Advanced Composites USA, Inc.), and then joined with the A-CNT network that is adhered onto GNPT (see Figure 2b) ensuring that the CNT alignment is perpendicular to the length of the Cu mesh. This heater architecture has two primary advantages for

resistive curing: (1) the surfacing film leads to a cured material that has both low porosity and surface roughness; (2) the high resistivity of the surfacing film ensures that the A-CNT film is electrically, but not thermally, insulated from the surface of the material that will be cured, ensuring that electron transport is sequestered to the A-CNT film (for use in Joule heating), and thereby enabling the formation of a uniform and tailorable temperature profile. Additional details can be found elsewhere.[50]

Degree of Cure Testing. Degree of cure testing was performed on a 40 mm × 50 mm 16-ply unidirectional carbon fiber laminate following the vacuum bag scheme detailed in the Cycom 5320-1 (Cytec Industries, Inc.) technical data sheet (these details can also be found in ref 50). The following cure cycle was used for both the oven cured baseline, and the samples cured using the A-CNT film heater: ramp rate of $0.6-2.8^{\circ}$C/min; cure temperature of $121 \pm 6^{\circ}$C with a hold time of 3 hr; and post cure temperature of 177°C with a hold time of 2 hr. Since the aligned CNT film heater on the laminate was heated by Joule heating, the DC power supply($\sim$ 30 V) was directly connected to two electrodes of CNT film heater. By manual adjustment of input voltage, the average temperature of CNT film heater followed the selected cure cycle. Input voltage and current were recorded *via* a digital multimeter (Hewlett Packard 34401A) with alligator clips every 0.3 s. Thermography was taken using a thermal camera (PCE-TC 3 from PCE Group) every 6 seconds, and the average temperature of CNT film heater was calculated from the temperature data in the area between two parallel electrodes. Once the cure was complete, differential scanning calorimetry (DSC) was used to evaluate the degree of cure (DoC) of the laminate by scanning up to 300°C. The degree of cure was calculated by comparing the area of the exothermic peak found in the DSC pattern of the heat treated laminate, commonly known as the heat of cure, to the heat of cure of a laminate that did not undergo heat treatment. In this analysis, a fully cured laminate would have a DoC of 100% (no exothermal peak), whereas an uncured laminate would have a DoC of 0%. Additional details can be found elsewhere.[50]

High Temperature Testing. The maximum operating temperature of the A-CNT film

heater was determined in ambient air using a microheater measuring ~ 15 mm $\times \sim 15$ mm on a quartz substrate. The maximum temperature was recorded using a thermal camera (T640 from FLIR Systems, Inc.).

3 Results and Discussion

Thermal processing of PMCs requires the heater to follow a very precise manufacturer specified thermal profile. The electrothermal response of the A-CNT film heater during thermal processing can be split up into five stages (see Figure 3a). These five stages consist of three ramps stages (I, III, and IV), an initial cure stage (II) where polymer flow, gelation, and vitrification occurs, and a cure stage (IV) where polymer cross-linking occurs.[51] In Stage I, the temperature of the A-CNT film heater is ramped from room temperature to 121°C at a constant rate, and the heater resistance was observed to have a non-monotonic response of first decreasing from $\approx 13\ \Omega$ to $\approx 9\ \Omega$ then recovering to $\approx 10\ \Omega$, while the heater power increased monotonically from ≈ 0 W to ≈ 16 W. In this stage, the resistance of the CNT film first decreased due to the negative thermal coefficient of resistance (TCR) of the A-CNT network,[37] but then recovered at around 100°C due to capillary driven wetting of the A-CNT network by polymer found in the surfacing film.[52] This polymer infusion process leads to an increase in CNT-CNT junction resistance.[53] In Stage II, where the temperature was held at 121°C, the heater resistance increased monotonically from $\approx 10\ \Omega$ to $\approx 14\Omega$ due to continued flow of polymer from the surfacing film into the A-CNT network, while the heater power decreased from ≈ 16 W to ≈ 15 W due to the increase in heater resistance. In this stage, the polymer goes through two transitions:[51] gelation, where the polymer transforms from a liquid to a rubber like state;[54] and vitrification, where the polymer transforms from a rubber like state to a solid glassy state.[54] These transformations comprise the initial cure. To arrive at the cure temperature, Stage III consisted of a temperature ramp-up from 121°C to 177°C, and the heater resistance decreased from $\approx 14\ \Omega$ to $\approx 13\ \Omega$ (the TCR was lower

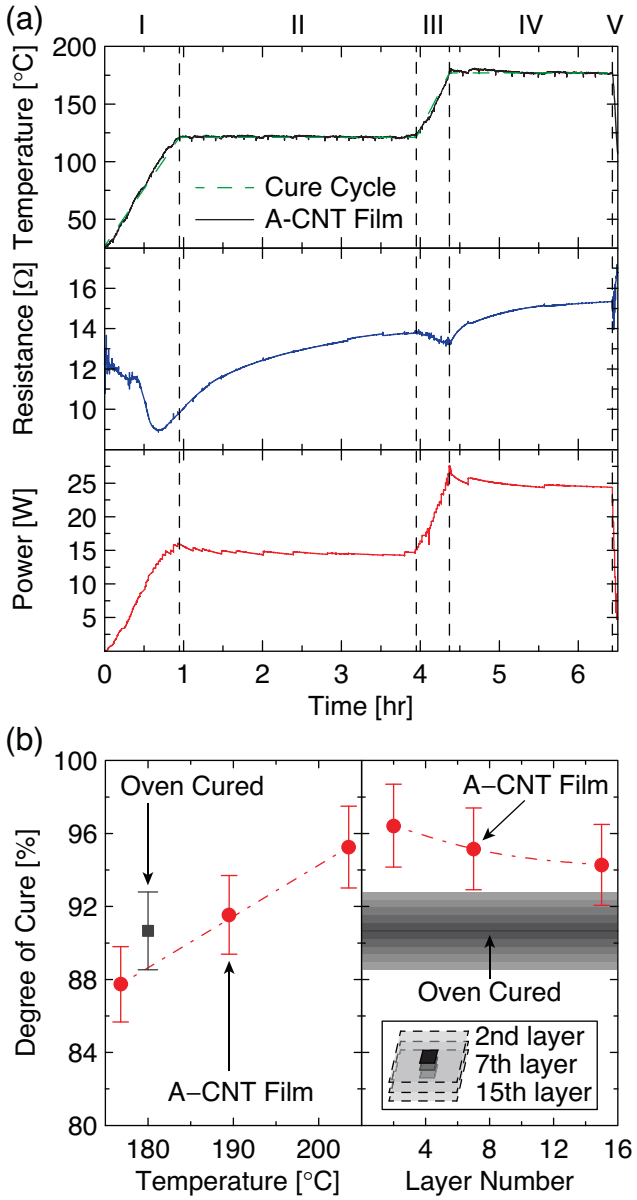

Figure 3: Performance of the A-CNT film heater during manufacturing. (a) A-CNT film heater temperature, resistance, and power during curing. The five stages of the composite manufacturing cycle are indicated. (b) Spatial variations in peak temperature in stage IV and the resulting degree of cure (100% corresponds to fully cured) for the 2nd, 7th, and 15th layer of the 16 layer composite.

due to polymer impregnation into the A-CNT network), while the heater power increased from $\approx$ 15 W to $\approx$ 28 W. The temperature was held at 177°C at Stage IV, where the heater resistance increased from $\approx$ 13 Ω to $\approx$ 15 Ω, and the heater power decreased from $\approx$ 28 W to $\approx$ 24 W due to the increased heater resistance. In this stage, the polymer undergoes cross-

linking that maximize the thermomechanical properties of the structure.[51] Stage V consisted of the post-thermal processing ramp down, and the heater resistance increased from $\approx 15\ \Omega$ to $\approx 18\ \Omega$ due to the negative TCR of the A-CNT film heater.[37] These observed changes in resistance and power during the thermal processing of the PMCs are a result of interactions between the A-CNT film heater and the polymer surfacing film, suggesting that the A-CNT film heater can act as a sensor during the formation of a polymer nanocomposite layer on the surface of the fabricated part.

To evaluate the quality of the thermal processing, and to determine whether the A-CNT film heater approach yields materials of equivalent quality, an analysis of the degree of cure (DoC) was performed (see Figure 3b).[50,55] As Figure 3b demonstrates, thermal processing with the A-CNT film heater leads to DoCs that are equivalent to or outperform (DoC $\approx 93\% - 99\%$) those obtained from the conventional oven technique (DoC $\approx 93\%$). Also, Figure 3b illustrates that the DoC of the laminate is strongly dependent on the surface temperature of the A-CNT film heater, which emphasizes the need for spatial control of heating. Since there should be no significant spatial variations in the temperature profile of the oven once steady state is reached, the DoC for the oven technique is only calculated at $\approx 180°C$ (the scaling of the DoC with cure temperature for oven based techniques can be found in Lee[50]). Note that the asymmetric and uninsulated fabrication setup (see Figure 2b) was purposefully designed to be the worst case scenario, and significant thermal losses were observed in the through-thickness direction of the laminate. This causes the degree of cure to decrease as a function of the ply number ($\propto$ the distance from the surface of the A-CNT film heater), although still exceeding the baseline (oven cured) DoC at 93% (see Figure 3b). Since the addition of insulation promises a more uniform thermal distribution and suppressed through-thickness thermal losses, future work on insulated asymmetric (a heater on one side) and symmetric (a heater on both sides) A-CNT film heater setups is planned, and will determine the maximum laminate thickness for which a uniform DoC throughout the whole composite can be obtained.

Previous studies have demonstrated that microheater films normally exhibit maximum operating temperatures of ≈ 100°C to 200°C, which severely limits the materials they could be used to process. As Figure 4 demonstrates, the A-CNT film heater used here is stable up to ≈ 550°C in ambient conditions (at 1 atm and ambient temperature of 25°C to simulate the worst case scenario), which is comparable to the best figures previously reported for CNT based electrothermal devices operating in air (~ 400°C for pristine CNTs, and ~ 700°C for SiC coated CNTs).[8,15,21,56] Since the A-CNT film heater could maintain such a high temperature for $\gtrapprox 1.5$ hr at a heater power of $\gtrapprox 20$ W/cm^{2}in this highly oxidizing environment, this microheater would see little degradation at $\lessapprox 550$°C during normal operation for part curing where the A-CNT film will either be in vacuum or not directly exposed to the ambient air. This means that the A-CNT film here reported here can be used for *in situ* thermal processing of high temperature polymers, such as polyacrylonitrile (PAN), polyimide, and poly(aryl ether ketone)s (*e.g.* PEEK and PEKK), which normally require temperatures of ~ 300°C to 400°C for processing.[57–62] Also, recent work has shown that CNT based heaters can be used at temperatures > 1000°C in non-oxidizing environments,[18,56] meaning that the A-CNT film heater reported here may be used for the low temperature carbonization step required for the synthesis of PAN based carbon fibers,[57] or the manufacture of other pyrolytic carbon based materials, such as aligned CNT carbon matrix nanocomposites.[38] These results indicate that with environmental control, the A-CNT film based microheaters could potentially be used to fabricate next-generation architectures comprised of both polymers and ceramics.

4 Conclusion

In summary, an aligned carbon nanotube (A-CNT) based microheater that is suitable for integration into existing and future multifunctional architectures was presented. The experimental results show that the A-CNT microheater film has a uniform surface temperature that can be tuned to accurately follow a temperature control profile. Because the laminates cured

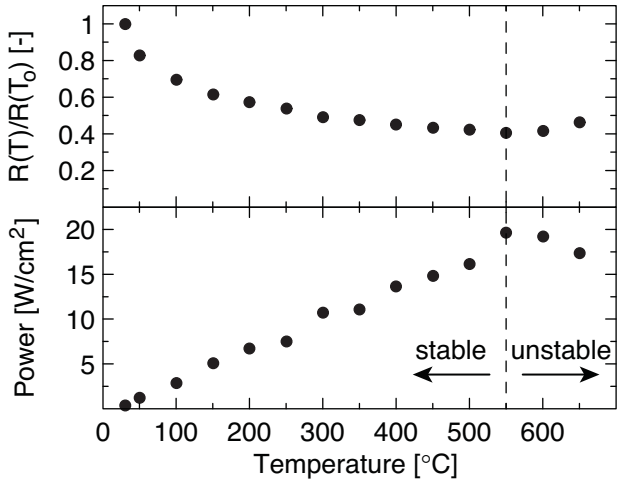

Figure 4: Temperature (T) response of the normalized resistance ($R(T)/R(T_\mathrm{o} = 30°\mathrm{C})$) and power density of the A-CNT film heater in ambient conditions on a quartz substrate illustrating that the maximum operating temperature of this device is $\gtrapprox 500°\mathrm{C}$.

by the A-CNT based microheater had a comparable degree of cure (DoC) to the laminates cured using a conventional oven based techniques, but required much less input energy (< 30 W peak for the A-CNT film heater vs. $\gtrsim 1$ KW peak for the oven), the microheater reported here can lead to orders of magnitude energy savings during processing of materials, consistent with the scaling analysis presented in Figure 1b. In the specific application presented here, energy for thermal processing of advanced composites accounts for $\sim 25 - 50\%$ of the total acquisition cost of such structures.[63] Also, since the A-CNT microheater film can operate at temperatures $> 500°\mathrm{C}$ in air and $> 1000°\mathrm{C}$ in non-oxidizing environments, this microheater can could be used for thermal processing of high temperature polymers, *e.g.* polyimides and polyaryletherketones, or low temperature pyrolysis of polymer derived ceramics. Since the experimental setup used here was for the worst case scenario (heater on one side with no insulation), future studies should explore the energy required for thermal processing of laminates in setups that incorporate insulation and multiple microheater films. Additionally, since the geometry of the part could affect the resulting temperature distribution, *e.g.* in areas of thickness variation such as ply drops and tapers, further work is planned to quantify the impact of laminate geometric variations on their DoC. Also, since thermal processing using the A-CNT film heater yields a multifunctional aligned-CNT polymer nanocompos-

ite layer on the composite surface, further work is required to explore the capabilities that may arise from the incorporation of such a nancomposite layer into polymeric structures. Using this microheater film, the design and manufacture of next-generation multifunctional architectures with built-in damage sensing and repairing capabilities may become possible.

Acknowledgement

This work was supported by Airbus Group, Boeing, Embraer, Lockheed Martin, Saab AB, TohoTenax, and ANSYS through MIT's Nano-Engineered Composite aerospace STructures (NECST) Consortium and was supported (in part) by AFRL/RX contract FA8650-11-D-5800, Task Order 0003, and was supported (in part) by the U.S. Army Research Office under contract W911NF-07-D-0004 and W911NF-13-D-0001. J.L. acknowledges support from the Kwanjeong Educational Foundation. I.Y.S. was supported by the Department of Defense (DoD) through the National Defense Science & Engineering Graduate Fellowship (NDSEG) Program. S.S.K. acknowledges support from Naval Sea Systems Command contract N00024-12-P-4069 for SBIR topic N121-058. The authors thank the Air Force Research Lab (AFRL) at Wright Patterson Air Force Base (WPAFB) for materials donation and Dr. Jeffery W. Baur (AFRL) and Dr. Brent L. Volk (AFRL) for technical assistance with the out-of-autoclave material, Dr. Sunny S. Wicks (MIT), John Kane (MIT) and the entire necstlab at MIT for technical support and advice. This work made use of the core facilities at the Institute for Soldier Nanotechnologies at MIT, supported in part by the U.S. Army Research Office under contract W911NF-07-D-0004, and was carried out in part through the use of MIT's Microsystems Technology Laboratories.

References

(1) Wojtecki, R. J.; Meador, M. A.; Rowan, S. J. Using the Dynamic Bond to Access Macroscopically Responsive Structurally Dynamic Polymers. *Nat. Mater.* **2011**, *10*, 14–27.

(2) Burattini, S.; Greenland, B. W.; Chappell, D.; Colquhoun, H. M.; Hayes, W. Healable Polymeric Materials: A Tutorial Review. *Chem. Soc. Rev.* **2010**, *39*, 1973–1985.

(3) Hager, M. D.; Greil, P.; Leyens, C.; van der Zwaag, S.; Schubert, U. S. Self-Healing Materials. *Adv. Mater.* **2010**, *22*, 5424–5430.

(4) Hammock, M. L.; Chortos, A.; Tee, B. C.-K.; Tok, J. B.-H.; Bao, Z. 25th Anniversary Article: The Evolution of Electronic Skin (E-Skin): a Brief History, Design Considerations, and Recent Progress. *Adv. Mater.* **2013**, *25*, 5997–6038.

(5) Yan, X.; Wang, F.; Zheng, B.; Huang, F. Stimuli-Responsive Supramolecular Polymeric Materials. *Chem. Soc. Rev.* **2012**, *41*, 6042–6065.

(6) Wool, R. P. Self-Healing Materials: A Review. *Soft Matter* **2008**, *4*, 400–418.

(7) Yoon, Y.-H.; Song, J.-W.; Kim, D.; Kim, J.; Park, J.-K.; Oh, S.-K.; Han, C.-S. Transparent Film Heater Using Single-Walled Carbon Nanotubes. *Adv. Mater.* **2007**, *19*, 4284–4287.

(8) Wu, Z. P.; Wang, J. N. Preparation of Large-Area Double-Walled Carbon Nanotube Films and Application As Film Heater. *Physica E* **2009**, *42*, 77 – 81.

(9) Kim, D.; Lee, H.-C.; Woo, J. Y.; Han, C.-S. Thermal Behavior of Transparent Film Heaters Made of Single-Walled Carbon Nanotubes. *J. Phys. Chem. C* **2010**, *114*, 5817–5821.

(10) Kang, J.; Kim, H.; Kim, K. S.; Lee, S.-K.; Bae, S.; Ahn, J.-H.; Kim, Y.-J.; Choi, J.-B.; Hong, B. H. High-Performance Graphene-Based Transparent Flexible Heaters. *Nano Lett.* **2011**, *11*, 5154–5158.

(11) Jiang, K.; Wang, J.; Li, Q.; Liu, L.; Liu, C.; Fan, S. Superaligned Carbon Nanotube Arrays, Films, and Yarns: A Road to Applications. *Adv. Mater.* **2011**, *23*, 1154–1161.

(12) Jang, H.-S.; Jeon, S. K.; Nahm, S. H. The Manufacture of a Transparent Film Heater by Spinning Multi-Walled Carbon Nanotubes. *Carbon* **2011**, *49*, 111 – 116.

(13) Liu, P.; Liu, L.; Jiang, K.; Fan, S. Carbon-Nanotube-Film Microheater on a Polyethylene Terephthalate Substrate and Its Application in Thermochromic Displays. *Small* **2011**, *7*, 732–736.

(14) Im, H.; Jang, E. Y.; Choi, A.; Kim, W. J.; Kang, T. J.; Park, Y. W.; Kim, Y. H. Enhancement of Heating Performance of Carbon Nanotube Sheet with Granular Metal. *ACS Appl. Mater. Interfaces* **2012**, *4*, 2338–2342.

(15) Janas, D.; Koziol, K. K. Rapid Electrothermal Response of High-Temperature Carbon Nanotube Film Heaters. *Carbon* **2013**, *59*, 457 – 463.

(16) Jung, D.; Han, M.; Lee, G. S. Flexible Transparent Conductive Heater Using Multi-walled Carbon Nanotube Sheet. *J. Vac. Sci. Technol., B: Nanotechnol. Microelectron.: Mater., Process., Meas., Phenom.* **2014**, *32*, 04E105.

(17) Chu, H.; Zhang, Z.; Liu, Y.; Leng, J. Self-Heating Fiber Reinforced Polymer Composite Using Meso/macropore Carbon Nanotube Paper and Its Application in Deicing. *Carbon* **2014**, *66*, 154 – 163.

(18) Aliev, A. E.; Mayo, N. K.; Baughman, R. H.; Avirovik, D.; Priya, S.; Zarnetske, M. R.; Blottman, J. B. Thermal Management of Thermoacoustic Sound Projectors Using a Free-Standing Carbon Nanotube Aerogel Sheet As a Heat Source. *Nanotechnology* **2014**, *25*, 405704.

(19) Sorel, S.; Bellet, D.; Coleman, J. N. Relationship Between Material Properties and Transparent Heater Performance for Both Bulk-like and Percolative Nanostructured Networks. *ACS Nano* **2014**, *8*, 4805–4814.

(20) Bae, J. J.; Lim, S. C.; Han, G. H.; Jo, Y. W.; Doung, D. L.; Kim, E. S.; Chae, S. J.; Huy, T. Q.; Van Luan, N.; Lee, Y. H. Heat Dissipation of Transparent Graphene Defoggers. *Adv. Funct. Mater.* **2012**, *22*, 4819–4826.

(21) Janas, D.; Koziol, K. K. A Review of Production Methods of Carbon Nanotube and Graphene Thin Films for Electrothermal Applications. *Nanoscale* **2014**, *6*, 3037–3045.

(22) Du, J.; Pei, S.; Ma, L.; Cheng, H.-M. 25th Anniversary Article: Carbon Nanotube- and Graphene-Based Transparent Conductive Films for Optoelectronic Devices. *Adv. Mater.* **2014**, *26*, 1958–1991.

(23) Menzel, R.; Barg, S.; Miranda, M.; Anthony, D. B.; Bawaked, S. M.; Mokhtar, M.; Al-Thabaiti, S. A.; Basahel, S. N.; Saiz, E.; Shaffer, M. S. P. Joule Heating Characteristics of Emulsion-Templated Graphene Aerogels. *Adv. Funct. Mater.* **2015**, *25*, 28–35.

(24) Kim, T.; Kim, Y. W.; Lee, H. S.; Kim, H.; Yang, W. S.; Suh, K. S. Uniformly Interconnected Silver-Nanowire Networks for Transparent Film Heaters. *Adv. Funct. Mater.* **2013**, *23*, 1250–1255.

(25) Han, B.; Pei, K.; Huang, Y.; Zhang, X.; Rong, Q.; Lin, Q.; Guo, Y.; Sun, T.; Guo, C.; Carnahan, D.; Giersig, M.; Wang, Y.; Gao, J.; Ren, Z.; Kempa, K. Uniform Self-Forming Metallic Network As a High-Performance Transparent Conductive Electrode. *Adv. Mater.* **2014**, *26*, 873–877.

(26) Gupta, R.; Rao, K. D. M.; Srivastava, K.; Kumar, A.; Kiruthika, S.; Kulkarni, G. U. Spray Coating of Crack Templates for the Fabrication of Transparent Conductors and Heaters on Flat and Curved Surfaces. *ACS Appl. Mater. Interfaces* **2014**, *6*, 13688–13696.

(27) Chang, Y.-M.; Yeh, W.-Y.; Chen, P.-C. Highly Foldable Transparent Conductive Films Composed of Silver Nanowire Junctions Prepared by Chemical Metal Reduction. *Nanotechnology* **2014**, *25*, 285601.

(28) Ji, S.; He, W.; Wang, K.; Ran, Y.; Ye, C. Thermal Response of Transparent Silver Nanowire/PEDOT:PSS Film Heaters. *Small* **2014**, *10*, 4951–4960.

(29) Rao, K. D. M.; Gupta, R.; Kulkarni, G. U. Fabrication of Large Area, High-Performance, Transparent Conducting Electrodes Using a Spontaneously Formed Crackle Network As Template. *Adv. Mater. Interfaces* **2014**, *1*, 1400090.

(30) Rao, K. D. M.; Kulkarni, G. U. A Highly Crystalline Single Au Wire Network As a High Temperature Transparent Heater. *Nanoscale* **2014**, *6*, 5645–5651.

(31) Zhang, X.; Yan, X.; Chen, J.; Zhao, J. Large-Size Graphene Microsheets As a Protective Layer for Transparent Conductive Silver Nanowire Film Heaters. *Carbon* **2014**, *69*, 437 – 443.

(32) Woo, J. Y.; Kim, K. K.; Lee, J.; Kim, J. T.; Han, C.-S. Highly Conductive and Stretchable Ag Nanowire/carbon Nanotube Hybrid Conductors. *Nanotechnology* **2014**, *25*, 285203.

(33) Wang, D.; Song, P.; Liu, C.; Wu, W.; Fan, S. Highly Oriented Carbon Nanotube Papers Made of Aligned Carbon Nanotubes. *Nanotechnology* **2008**, *19*, 075609.

(34) Zhang, L.; Zhang, G.; Liu, C.; Fan, S. High-Density Carbon Nanotube Buckypapers with Superior Transport and Mechanical Properties. *Nano Lett.* **2012**, *12*, 4848–4852.

(35) Chen, G.; Futaba, D. N.; Sakurai, S.; Yumura, M.; Hata, K. Interplay of Wall Number and Diameter on the Electrical Conductivity of Carbon Nanotube Thin Films. *Carbon* **2014**, *67*, 318 – 325.

(36) Marschewski, J.; In, J. B.; Poulikakos, D.; Grigoropoulos, C. P. Synergistic Integration of Ni and Vertically Aligned Carbon Nanotubes for Enhanced Transport Properties on Flexible Substrates. *Carbon* **2014**, *68*, 308 – 318.

(37) Lee, J.; Stein, I. Y.; Devoe, M. E.; Lewis, D. J.; Lachman, N.; Kessler, S. S.; Bushhorn, S. T.; Wardle, B. L. Impact of Carbon Nanotube Length on Electron Transport in Aligned Carbon Nanotube Films. *Appl. Phys. Lett.* **2015**, *106*, 053110.

(38) Stein, I. Y.; Wardle, B. L. Morphology and Processing of Aligned Carbon Nanotube Carbon Matrix Nanocomposites. *Carbon* **2014**, *68*, 807 – 813.

(39) Buschhorn, S. T.; Kessler, S. S.; Lachman, N.; Gavin, J.; Thomas, G.; Wardle, B. L. *54th AIAa Structures, Structural Dynamics, and Materials (SDM) Conference*; 2013.

(40) Thostenson, E.; Chou, T.-W. Microwave Processing: Fundamentals and Applications. *Composites, Part A* **1999**, *30*, 1055 – 1071.

(41) Papargyris, D.; Day, R.; Nesbitt, A.; Bakavos, D. Comparison of the Mechanical and Physical Properties of a Carbon Fibre Epoxy Composite Manufactured by Resin TransferMoulding Using Conventional and Microwave Heating. *Compos. Sci. Technol.* **2008**, *68*, 1854 – 1861.

(42) Li, N.; Li, Y.; Hang, X.; Gao, J. Analysis and Optimization of Temperature Distribution in Carbon Fiber Reinforced Composite Materials During Microwave Curing Process. *J. Mater. Process. Technol.* **2014**, *214*, 544 – 550.

(43) Li, N.; Li, Y.; Hao, X.; Gao, J. A Comparative Experiment for the Analysis of Microwave and Thermal Process Induced Strains of Carbon Fiber/Bismaleimide Composite Materials. *Compos. Sci. Technol.* **2015**, *106*, 15 – 19.

(44) Wardle, B. L.; Saito, D. S.; García, E. J.; Hart, A. J.; Guzmán de Villoria, R.; Verploegen, E. A. Fabrication and Characterization of Ultrahigh-Volume- Fraction Aligned Carbon Nanotube Polymer Composites. *Adv. Mater.* **2008**, *20*, 2707–2714.

(45) Marconnet, A. M.; Yamamoto, N.; Panzer, M. A.; Wardle, B. L.; Goodson, K. E.

Thermal Conduction in Aligned Carbon Nanotube-Polymer Nanocomposites with High Packing Density. *ACS Nano* **2011**, *5*, 4818–4825.

(46) Stein, I. Y.; Wardle, B. L. Coordination Number Model to Quantify Packing Morphology of Aligned Nanowire Arrays. *Phys. Chem. Chem. Phys.* **2013**, *15*, 4033–4040.

(47) Hart, A. J.; Slocum, A. H. Rapid Growth and Flow-Mediated Nucleation of Millimeter-Scale Aligned Carbon Nanotube Structures from a Thin-Film Catalyst. *J. Phys. Chem. B* **2006**, *110*, 8250–8257.

(48) Stein, I. Y.; Lachman, N.; Devoe, M. E.; Wardle, B. L. Exohedral Physisorption of Ambient Moisture Scales Non-Monotonically with Fiber Proximity in Aligned Carbon Nanotube Arrays. *ACS Nano* **2014**, *8*, 4591–4599.

(49) Mitchell, R. R.; Yamamoto, N.; Cebeci, H.; Wardle, B. L.; Thompson, C. V. A Technique for Spatially-Resolved Contact Resistance-Free Electrical Conductivity Measurements of Aligned-Carbon Nanotube/polymer Nanocomposites. *Compos. Sci. Technol.* **2013**, *74*, 205 – 210.

(50) Lee, J. *in Situ* Curing of Polymeric Composites *via* Resistive Heaters Comprised of Aligned Carbon Nanotube Networks. M.Sc. thesis, Massachusetts Institute of Technology, Cambridge, Massachusetts, U.S.A., 2014.

(51) Centea, T.; Grunenfelder, L.; Nutt, S. A Review of Out-Of-Autoclave Prepregs - Material Properties, Process Phenomena, and Manufacturing Considerations. *Composites, Part A* **2015**, *70*, 132 – 154.

(52) García, E. J.; Hart, A. J.; Wardle, B. L.; Slocum, A. H. Fabrication of Composite Microstructures by Capillarity-Driven Wetting of Aligned Carbon Nanotubes with Polymers. *Nanotechnology* **2007**, *18*, 165602.

(53) Qiu, J.; Terrones, J.; Vilatela, J. J.; Vickers, M. E.; Elliott, J. A.; Windle, A. H. Liquid Infiltration into Carbon Nanotube Fibers: Effect on Structure and Electrical Properties. *ACS Nano* **2013**, *7*, 8412–8422.

(54) Vora, K.; Vo, T.; Islam, M.; Habibi, M.; Minaie, B. Evolution of Mechanical Properties During Cure for Out-Of-Autoclave Carbon-Epoxy Prepregs. *J. Appl. Polym. Sci.* **2015**, *132*, 41548.

(55) Yousefi, A.; Lafleur, P. G.; Gauvin, R. Kinetic Studies of Thermoset Cure Reactions: A Review. *Polym. Compos.* **1997**, *18*, 157–168.

(56) Park, J. G.; Li, S.; Liang, R.; Fan, X.; Zhang, C.; Wang, B. The High Current-Carrying Capacity of Various Carbon Nanotube-Based Buckypapers. *Nanotechnology* **2008**, *19*, 185710.

(57) Yu, M.; Wang, C.; Zhao, Y.; Zhang, M.; Wang, W. Thermal Properties of Acrylonitrile/itaconic Acid Polymers in Oxidative and Nonoxidative Atmospheres. *J. Appl. Polym. Sci.* **2010**, *116*, 1207–1212.

(58) Xue, Y.; Liu, J.; Liang, J. Kinetic Study of the Dehydrogenation Reaction in Polyacrylonitrile-Based Carbon Fiber Precursors During Thermal Stabilization. *J. Appl. Polym. Sci.* **2013**, *127*, 237–245.

(59) Chen, Y.; Lin, B.; Yang, H.; Zhang, X.; Sun, Y. Influence of Curing Temperature on Properties of the Polyacrylonitrile/polyimide Composite Films. *J. Appl. Polym. Sci.* **2014**, *131*, 40283.

(60) Saeed, M.; Zhan, M.-S. Effects of Monomer Structure and Imidization Degree on Mechanical Properties and Viscoelastic Behavior of Thermoplastic Polyimide Films. *Eur. Polym. J.* **2006**, *42*, 1844 – 1854.

(61) Shin, T. J.; Ree, M. Thermal Imidization and Structural Evolution of Thin Films of Poly(4,4-Oxydiphenylene P-Pyromellitamic Diethyl Ester). *J. Phys. Chem. B* **2007**, *111*, 13894–13900.

(62) Manolakis, I.; Cross, P.; Ward, S.; Colquhoun, H. M. Ring-Opening Polymerization in Molten PEEK: Transient Reduction of Melt-Viscosity by Macrocyclic Aromatic Thioetherketones. *J. Mater. Chem.* **2012**, *22*, 20458–20464.

(63) Eaglesham, M. A. A Decision Support System for Advanced Composites Manufacturing Cost Estimation. Ph.D. thesis, Virginia Polytechnic Institute and State University, Blacksburg, Virginia, U.S.A., 1998.